Journal of Solution Chemistry
https://doi.org/10.1007/s10953-023-01352-6

Evaluation of Thermodynamic Model of Pd(II) Complex Formation with Isosaccharinic Acid

Shingo Kimuro[1] · Yayoi Taneichi[1] · Hajime Iwata[1] · Takamitsu Ishidera[1] · Akira Kitamura[1] · Yukio Tachi[1] · Takeru Tanaka[2] · Kana Hirano[2] · Manami Hieda[2] · Shunsuke Miyabe[2] · Daisuke Kawamoto[3]

Received: 15 June 2023 / Accepted: 1 December 2023

Abstract
Palladium-107 is one of the selected radionuclides in the safety assessment of geological disposal of radioactive waste. Although isosaccharinic acid (ISA) forms strong complexes with many elements and enhances element solubility, the thermodynamic evaluation of the complex of Pd with ISA has not been conducted. In this study, the solubility of $Pd(OH)_2$ at pH 8.5–12.5 in the presence of ISA was investigated under inert gas (N_2) atmosphere. Furthermore, the coordination state of aqueous Pd and ISA was investigated by X-ray absorption and Fourier transform infrared spectroscopy, respectively. According to experimental results, the number of OH ligands in the mixed complex depends on pH. The thermodynamic model and conditional equilibrium constants of the Pd-ISA complex were estimated by slope analyses of solubility experiments at different pH levels and ionic strengths based on the specific ion interaction theory. Hence, the impact of complexation with ISA on Pd(II) solubility under disposal conditions could be quantified using the proposed thermodynamic models in this study.

Keywords Palladium(II) · Isosaccharinic acid (ISA) · Complexation · Thermodynamics · Specific ion interaction theory (SIT)

1 Introduction

Palladium-107 (^{107}Pd) is one of the selected radionuclides for the safety assessment of geological disposal of radioactive wastes by Nuclear Waste Management Organization of Japan (NUMO), which is the organization in charge of implementing safe geological

✉ Takamitsu Ishidera
ishidera.takamitsu@jaea.go.jp

[1] Nuclear Fuel Cycle Engineering Laboratories, Japan Atomic Energy Agency, 4-33 Muramatsu, Tokai-mura, Naka-gun, Ibaraki 319-1194, Japan

[2] Environment Department, Kyudensangyo CO., INC, 2-18-20 Najima, Higashi-ku, Fukuoka 813-0043, Japan

[3] Department of Chemistry, Faculty of Science, Okayama University of Science, 1-1 Ridaicho, Kita-ku, Okayama 700-0005, Japan

Published online: 17 January 2024

disposal of high-level radioactive waste and a part of TRU waste in Japan [1]. Some part of TRU waste contains organic materials such as cellulose, ion exchange resin, cement additives, etc. In highly alkaline cement porewaters, cellulose is degraded to low molecular weight compounds, and α-isosaccharinic acid (ISA) should be the final product in the presence of Ca^{2+} [2–4]. As a result, ISA is considered one of the main representatives of polyhydroxy carboxylic acids, which could form stable complexes with various metal cations [5–7] expected in cementitious environments, such as the disposal site of radioactive wastes. For this reason, OECD/NEA selected ISA as one of the target organic ligands in the thermodynamic database [8].

The Pd^{2+} ion is one of the most strongly hydrolyzed cations [9]; however, there is a possibility that the complex formation with ISA may enhance the solubility of Pd hydroxide. Nevertheless, only a limited number of experimental investigations have been conducted to determine the thermodynamic values on hydrolysis and complexation with organic ligands of palladium even though the prediction of palladium dissolution and/or migration behavior in geologic environments is necessary in the safety assessment. Middlesworth et al. [10] reported thermodynamic data for hydroxide and mixed hydroxy-chloride of Pd by solubility experiments, which were conducted over a range of pH, temperature, and ionic strength. Oda et al. [11] conducted a solubility experiment on Pd under anaerobic conditions and then estimated that Pd metal may be the solubility-limiting solid phase under repository conditions and that the solubility of Pd metal should be $< 10^{-9}$ mol·dm^{-3}. Rai et al. [12] recommended some equilibrium constants and specific ion interaction theory (SIT) parameters by reviewing published values for thermodynamic models for amorphous $Pd(OH)_2$ solubility in Pd–OH and Pd–Cl systems.

Although thermodynamic data of the interaction of Pd(II) with ISA are essential for nuclide migration analysis (i.e., setting robust upper limit values of the aqueous Pd(II) concentration in the direct vicinity of the waste packages) of Pd(II) in the safety assessment of geological disposal and the evaluation of impact of ISA complexation on the solubility, reliable thermodynamic models, and complexation constants have not been reported. Therefore, in this study, complex species and constants of Pd-ISA were estimated through batch solubility experiments under neutral–alkaline pH conditions. Furthermore, the structure of complex molecules was analyzed by Fourier transform infrared spectroscopy (FTIR) and X-ray absorption (XA) spectroscopy. Consequently, accurate determination of thermodynamic values for the complex of Pd(II) with ISA could be achieved.

2 Experimental

2.1 Chemicals

All solutions were prepared with ultrapure water (RFU667HA, ADVANTEC). A commercial $PdCl_2$ powder (98%, Wako Pure Chemicals) was used without purification. 2.66 g of powder was dissolved in 100 ml of a 0.02 mol·dm^{-3} NaCl solution by adding 3 ml of conc. HCl; then, it was used as a stock solution of Pd (II). An ISA solution was prepared with sodium salt, converted from purchased calcium salt (98%, Alfa Aesar) by the following procedure. 4.79 g of ISA calcium salt powder was dissolved in 200 ml of 0.35 mol·dm^{-3} Na_2CO_3 with a 0.01 mol·dm^{-3} NaOH solution and mixed using a magnetic stirrer for 16 h. Then, the precipitate was separated by centrifugation (3600 rpm/60 min) to remove Ca as $CaCO_3$. The supernatant solution was collected in a vessel and moved to a glovebox filled

with N_2. The aliquot of the HCl solution was added until pH decreased to 4.8, and the dissolved carbonate was removed by bubbling N_2 for 2 h. Finally, the pH of the solution was adjusted by adding 8 mol·dm^{-3} NaOH, and the concentration of the ISA stock solution was calculated to be approximately 0.1 mol·dm^{-3}.

2.2 Solubility Experiment

Batch solubility experiments were conducted under saturated conditions with synthesized solids of Pd hydroxide. All experiments were conducted in N_2 atmosphere. The Pd (II) stock solutions were diluted by the NaCl solution for setting the ionic strength to 0.1 or 0.6 mol·dm^{-3}, and then, the solution pH was adjusted to 8.5 or 10 by NaOH addition. The visible amount of Pd solid was observed and stored for 14 days. After the sampling of initial solution, ISA solution was added and pH was adjusted to about 8.5, 10.5, and 12.5 using NaOH and HCl, respectively. The total concentration of Pd was 3.0×10^{-3} mol·dm^{-3}, with that of ISA in the range of 10^{-4}–10^{-2} mol·dm^{-3}. After each experimental period (up to 56 days), the pH of the solution was measured using a pH meter (D-71, HORIBA) with a calibrated combined glass electrode (9615 S, HORIBA). Then, the solution was separated from the solid by ultrafiltration through a 10,000-molecular weight cutoff polysulfone filter unit (PT-1004, APRO Science). The Pd concentration in the filtrates was determined by inductively coupled plasma-mass spectrometry (Agilent 7900), with a quantitative detection limit of 1.0×10^{-8} mol·dm^{-3} (maximum value of 10 sigma of repeated blank measurements). The aqueous concentration of ISA was determined by the non-purgeable organic carbon (NPOC) method using a total organic carbon analyzer (Sievers 900, GE Analytical Instruments). The batch experiments were repeated at least twice.

2.3 Pd K-edge XA Spectroscopy

For XA spectra measurements, Pd-ISA solutions with different ISA/Pd mole ratios were prepared, and the pH of the solutions was adjusted to 8.5, 10, and 12.5 (Table 1). In addition, a Pd-ISA solution ([ISA]/[Pd] = 3.3) at pH 3.8 was prepared to investigate the relationship between the formation of an aqueous Pd-ISA complex and the deprotonation of the carboxyl group of ISA ($pK_a = 3.27$ [13]).

Pd K-edge XA spectra for the Pd-ISA solutions and standard materials (K_2PdCl_4, $[PdCl_4]^{2-}$ solution, PdO, $[Pd(OH)_4]^{2-}$ solution, $Pd(CH_3COO)_2$, and $[Pd(CH_3COO)_2]$ solution) were recorded at BL14B2 of SPring-8 (Hyogo, Japan) using a Si(311) double crystal monochromator. Solid samples were diluted with boron nitride, made into pellets, and placed in a polyethylene bag.

All XA spectra data for all samples were recorded under ambient conditions in transmission mode, and the transmitted X-ray was detected using an ion chamber. Spectral analysis

Table 1 Pd-ISA solutions for XA spectra measurement

	[ISA]/mol·dm^{-3}	[Pd]/mol·dm^{-3}	pH
Pd-ISA solution ([ISA]/[Pd] = 1)	6.0×10^{-2}	6.0×10^{-2}	8.5, 10.0 and 12.5
Pd-ISA solution ([ISA]/[Pd] = 2)	6.0×10^{-2}	3.0×10^{-2}	8.5, 10.0 and 12.5
Pd-ISA solution ([ISA]/[Pd] = 3.3)	1.0×10^{-2}	3.0×10^{-3}	3.8

was performed using Athena software [14]. The extraction of extended X-ray absorption fine structure (EXAFS) oscillation from the spectra, normalization by edge-jump, and Fourier transformation were performed using Athena software.

2.4 FTIR Analysis

A Fourier transform infrared spectrometer (SpotLight 400, Perkin Elmer) was used to characterize the aqueous Pd-ISA complex under different pH conditions. The measurements were performed in the attenuated total reflection (ATR) mode, and the instrument conditions were as follows: spectral range 1000–1800 cm^{-1}, resolution 1 cm^{-1}, and the number of scans 100. To investigate the effect of Pd on the ISA structure and the change in Pd-ISA complexes with pH, measurements were performed on the ISA stock solution and three different Pd-ISA solutions at pH 8.5,10, and 12.5. Pd-ISA solutions were prepared from the Pd and ISA stock solutions described above; the concentrations of both Pd and ISA were 6 $mmol{\cdot}dm^{-3}$ to obtain sufficient spectrum intensity. The solution pH was adjusted by adding HCl and NaOH.

3 Results and Discussion

3.1 Solubility of Pd(II) in the Presence of ISA

The experimentally measured Pd concentration as a function of contact time in the various concentration of ISA is depicted in Fig. 1(the concentration of ISA is shown in caption). A Pd concentration in 0 day indicates solubility in the absence of ISA, which is close to the quantitative detection limit of 1.0×10^{-8} $mol{\cdot}dm^{-3}$ in most cases. Middlesworth et al. reported the solubility of $Pd(OH)_2$ of approximately 1×10^{-7} $mol{\cdot}dm^{-3}$ at pH 8–10 through batch experiments under atmospheric conditions [10]. Conversely, Oda et al. reported that $Pd(OH)_2$ (am) gradually changed to crystalline Pd metal under anaerobic conditions, suggesting that the aqueous Pd concentration may be limited by Pd metal and may be less than 1×10^{-9} $mol{\cdot}dm^{-3}$ [11]. In this study, a visible amount of Pd hydroxide solid was precipitated and stored for 14 days in low-oxygen atmosphere. There are the variations in the initial Pd concentration in Fig. 1d–f, which may imply the precipitation had not been reached equilibrium in this ionic strength. The impact of oxygen concentration on the progress of conversion to Pd metal in this study is unclear; however, the aqueous concentrations of Pd were less than 1×10^{-7} $mol{\cdot}dm^{-3}$, even in the presence of 6×10^{-4} $mol{\cdot}dm^{-3}$ ISA at pH 8.5 and 10 of $I=0.1$ $mol{\cdot}dm^{-3}$. The dramatic increase in the Pd concentration in 7 days in Fig. 1 is caused by the addition of the ISA solution, implying that a soluble Pd-ISA complex is formed. In addition, the aqueous Pd concentration appeared to reach steady state values at 56 days. The values at pH 12.5 are likely to decrease with contact time, especially with low ISA concentrations. It is assumed that Pd hydroxide, immediately formed by the change in pH (10–12.5), should be converted to a stable Pd-ISA complex. Hereafter, Pd concentrations in 56 days, which are considered to be reaching equilibrium, were used for further discussion.

In Fig. 2, Pd(II) solubility at (a) $I=0.1$ and (b) 0.6 $mol{\cdot}dm^{-3}$ is shown as a function of aqueous ISA concentration, which was determined by NPOC. Pd(II) solubility increased with [ISA] with a slope of approximately 1, indicating that single ISA molecular was involved in the Pd-ISA complex. Additionally, an increase in solubility is evident in the

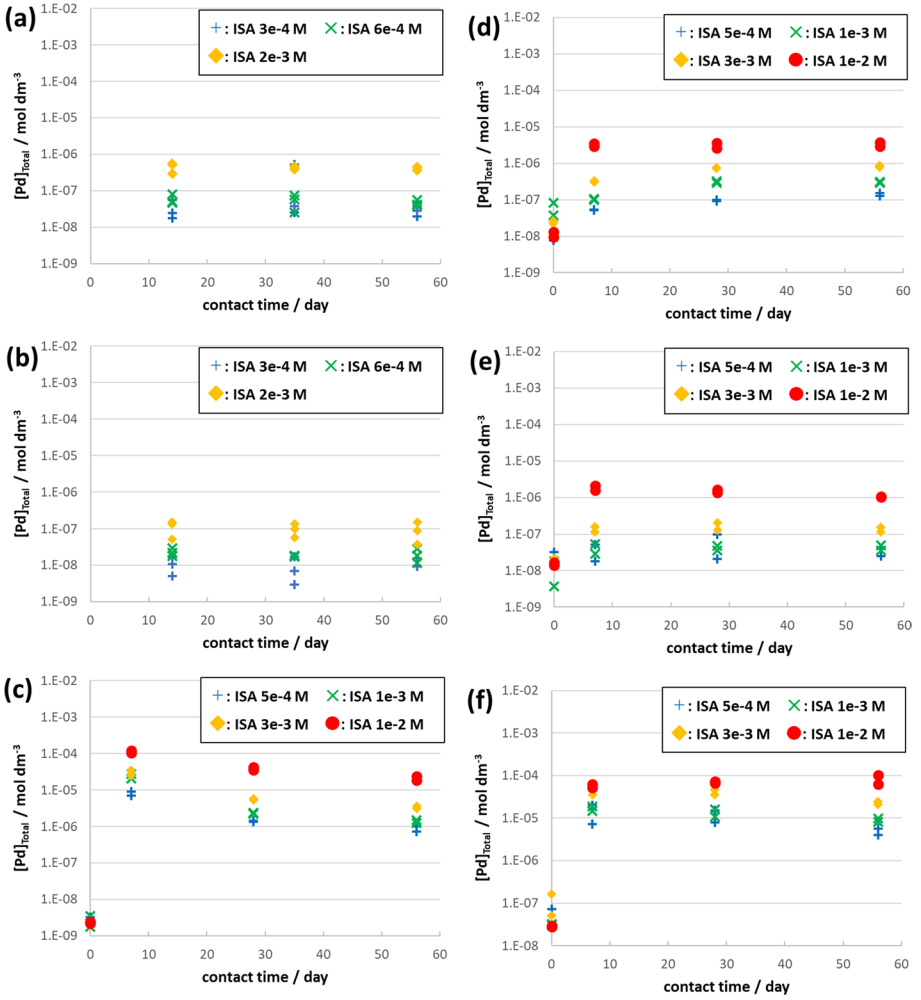

Fig. 1 Plot of aqueous Pd concentration vs. time of solution experiment in the presence of ISA at **a** pH 8.5, **b** pH 10, **c** pH 12.5 in $I = 0.1$ mol·dm^{-3}, **d** pH 8.5, **e** pH 10, and **f** pH 12.5 in $I = 0.6$ mol·dm^{-3}, respectively

following order: pH 12.5, 8.5, and 10. Considered soluble species of Pd are $Pd(OH)_2(aq)$, $Pd(OH)_3^-$, and Pd-ISA complex. The fraction of $Pd(OH)_3^-$ should increase with pH; however, the pH dependency of Pd solubility is not straightforward. This distinct pH dependency implies that the ternary complex species of Pd-OH-ISA are formed and the number of involved OH^- ions changes by pH.

3.2 XA Spectral Analysis of Aqueous Pd in the Presence of ISA

The XA spectra for K_2PdCl_4, $[PdCl_4]^{2-}$ solution, PdO, $[Pd(OH)_4]^{2-}$ solution, $Pd(CH_3COO)_2$, and $[Pd(CH_3COO)_2]$ solution were depicted in Supporting Information (Fig. S-1; Pd K-edge X-ray absorption near-edge structure (XANES) spectra, Fig. S-2;

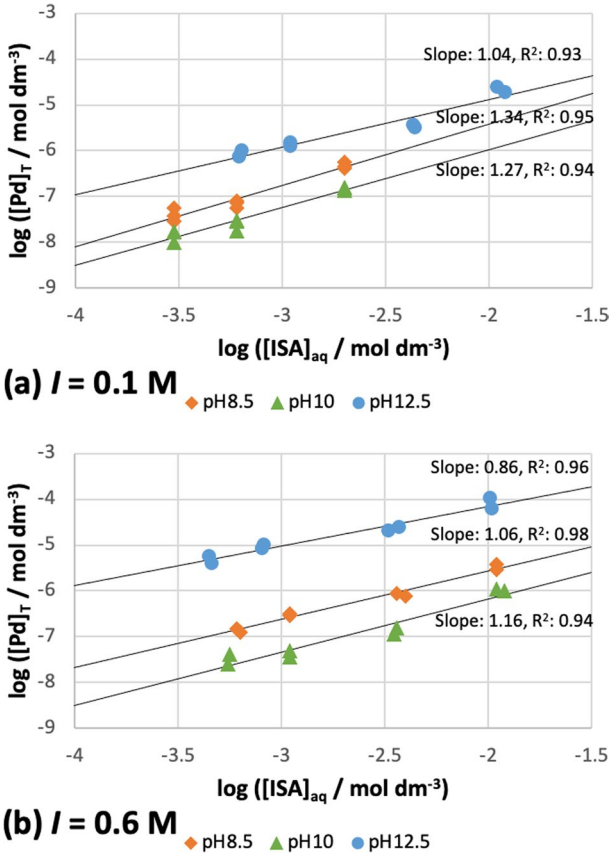

Fig. 2 Plot of experimental solubility data of aqueous Pd vs. ISA at **a** $I = 0.1$ mol·dm^{-3} and **b** $I = 0.6$ mol·dm^{-3}. The thin lines indicate the results of least-square fitting for each individual samples

k^3-weighted EXAFS oscillation extracted from Pd K-edge XA spectra, and Fig. S-3; Fourier transform of EXAFS oscillations extracted from Pd K-edge XA spectra). The shapes of XA spectra for K_2PdCl_4 and $Pd(CH_3COO)_2$ were similar to those for $[PdCl_4]^{2-}$ solution and $[Pd(CH_3COO)_2]$ solution, respectively. Therefore, it was suggested that the oxidation states and the geometries of $[PdCl_4]^{2-}$ solution and the $[Pd(CH_3COO)_2]$ solution are similar to those of K_2PdCl_4 and $Pd(CH_3COO)_2$, respectively. From the Fourier transforms of EXAFS oscillations extracted from Pd K-edge XA spectra for K_2PdCl_4 and $Pd(CH_3COO)_2$ (Fig. S-3), the peaks at 1.96 Å and 1.63 Å are assigned to the Pd-Cl and Pd-O interactions, respectively. Thus, the peaks at 1.84 Å of $[PdCl_4]^{2-}$ solution and 1.66 Å of $[Pd(CH_3COO)_2]$ solution are assigned to the Pd-Cl and Pd-O interactions, respectively. In addition, since the peak at 1.69 Å of PdO is assigned to Pd–O interaction, the peak at 1.66 Å of $[Pd(OH)_4]^{2-}$ solution is assigned to Pd–O interaction.

To examine the chemical state of aqueous Pd species in the presence of ISA, the Pd K-edge XA spectra for Pd-ISA solutions and standard materials were measured. Figure 3 depicts the Pd K-edge X-ray absorption near-edge structure (XANES) spectra for (a) a $[PdCl_4]^{2-}$ solution prepared by dissolving K_2PdCl_4 in a mixed solution of HCl (0.10 mol·dm^{-3}) and NaCl (2.0 mol·dm^{-3}), (b) a $[Pd(OH)_4]^{2-}$ solution prepared by dissolving K_2PdCl_4 in an 8.0 mol·dm^{-3} NaOH solution, (c) a $[Pd(CH_3COO)_2]$ solution

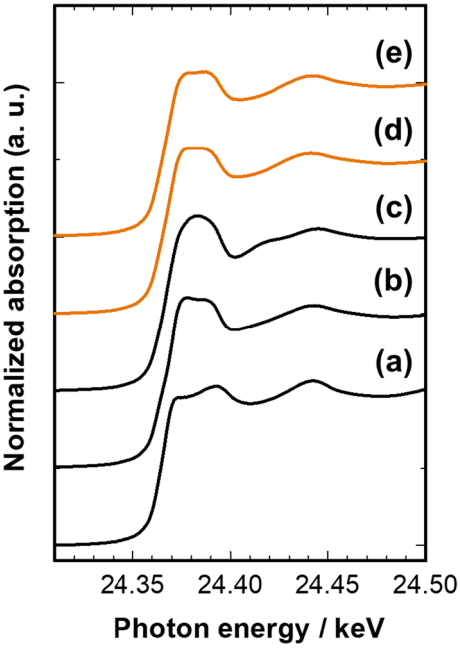

Fig. 3 Normalized Pd K-edge XANES spectra for **a** $[PdCl_4]^{2-}$ solution, **b** $[Pd(OH)_4]^{2-}$ solution, **c** $[Pd(CH_3COO)_2]$ solution, **d** Pd-ISA solution ([ISA]/[Pd] = 1, pH 8.5), and **e** Pd-ISA solution ([ISA]/[Pd] = 2, pH 8.5)

prepared by dissolving $Pd(CH_3COO)_2$ in toluene, (d) a Pd-ISA solution ([ISA]/[Pd] = 1, pH 8.5), and (e) a Pd-ISA solution ([ISA]/[Pd] = 2, pH 8.5).

As one of the coordination sites of ISA is the carboxyl group, the spectrum for the $[Pd(CH_3COO)_2]$ solution as a standard of Pd(II) with which the carboxyl group is coordinated was recorded. The shape of the spectrum for (d) the Pd-ISA solution ([ISA]/[Pd] = 1, pH 8.5) differed from that for (a) the $[PdCl_4]^{2-}$ solution as a standard of Pd(II) with which Cl^- is coordinated. Conversely, the shape of the spectrum for (d) the Pd-ISA solution ([ISA]/[Pd] = 1) was similar to those for (b) the $[Pd(OH)_4]^{2-}$ solution as a standard of Pd(II) that OH^- is coordinated with and (c) the $[Pd(CH_3COO)_2]$ solution. Furthermore, the shapes of the spectra for (d) the Pd-ISA solution ([ISA]/[Pd] = 1, pH 8.5) and (e) the Pd-ISA solution ([ISA]/[Pd] = 2, pH 8.5) were the same. As not shown here, the shapes of the spectra for the Pd-ISA solution at different pH levels were also the same. Figure 4 shows the EXAFS oscillation extracted from Pd K-edge XA spectra for (a) the $[PdCl_4]^{2-}$ solution, (b) the $[Pd(OH)_4]^{2-}$ solution, (c) the $[Pd(CH_3COO)_2]$ solution, (d) the Pd-ISA solution ([ISA]/[Pd] = 1, pH 8.5), and (e) the Pd-ISA solution ([ISA]/[Pd] = 2, pH 8.5).

The EXAFS oscillations for (d) the Pd-ISA solution ([ISA]/[Pd] = 1, pH 8.5) were out of phase with those for (b) the $[Pd(OH)_4]^{2-}$ and (c) $[Pd(CH_3COO)_2]$ solutions. It was suggested that the aqueous Pd species in the presence of ISA is the aqueous Pd-ISA complex. Furthermore, no difference was observed between the shapes of the EXAFS oscillations for (d) the Pd-ISA solution ([ISA]/[Pd] = 1, pH 8.5) and (e) the Pd-ISA solution ([ISA]/[Pd] = 2, pH 8.5). Therefore, it is considered that the molar ratio of ISA/Pd in the aqueous Pd-ISA complex is 1/1. To investigate atoms coordinated to Pd in the aqueous Pd-ISA complex, EXAFS oscillation analysis was performed. Fourier transforms of the EXAFS oscillations for (a) the $[PdCl_4]^{2-}$ solution, (b) the $[Pd(OH)_4]^{2-}$ solution, (c) the $[Pd(CH_3COO)_2]$ solution, (d) the Pd-ISA solution ([ISA]/[Pd] = 1, pH 8.5), and (e) the Pd-ISA solution ([ISA]/[Pd] = 2, pH 8.5) are depicted in Fig. 5. The peaks at 1.84 Å and 1.66

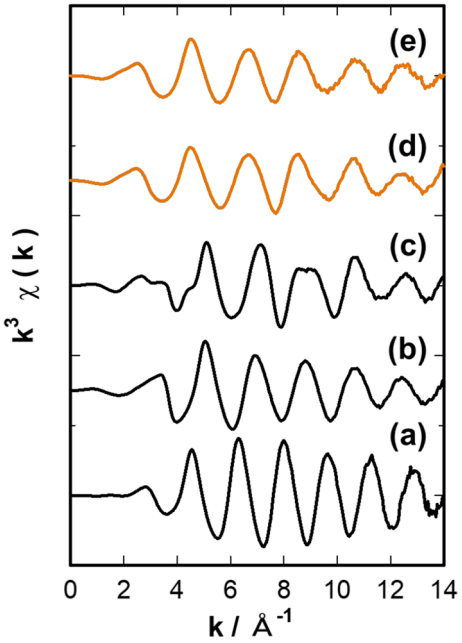

Fig. 4 k^3-weighted EXAFS oscillation extracted from Pd K-edge XA spectra for **a** $[PdCl_4]^{2-}$ solution, **b** $[Pd(OH)_4]^{2-}$ solution, **c** $[Pd(CH_3COO)_2]$ solution, **d** Pd-ISA solution ([ISA]/[Pd] = 1, pH 8.5), and **e** Pd-ISA solution ([ISA]/[Pd] = 2, pH 8.5)

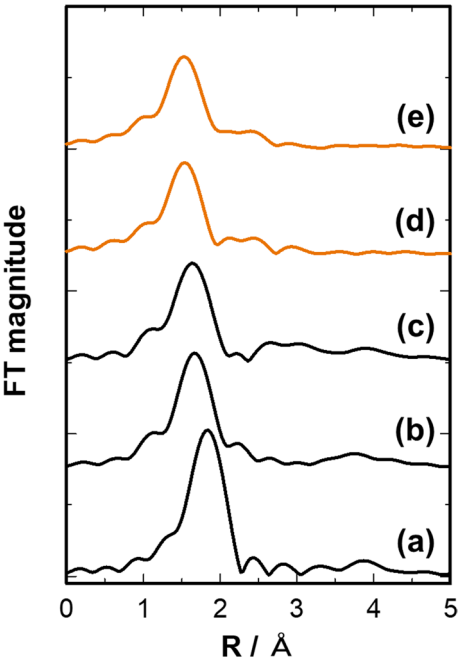

Fig. 5 Fourier transform of EXAFS oscillations extracted from Pd K-edge XA spectra for **a** $[PdCl_4]^{2-}$ solution, **b** $[Pd(OH)_4]^{2-}$ solution, **c** $[Pd(CH_3COO)_2]$ solution, **d** Pd-ISA solution ([ISA]/[Pd] = 1, pH 8.5), and **e** Pd-ISA solution ([ISA]/[Pd] = 2, pH 8.5)

Å are assigned to the Pd-Cl and Pd-O interactions, respectively. The peak at 1.53 Å of the aqueous Pd-ISA complex is attributed to the Pd–O interaction.

To investigate the relationship between the formation of the aqueous Pd-ISA complex and the deprotonation of the carboxyl group of ISA (pK_a = 3.27), the XA spectrum for the Pd-ISA solution ([ISA]/[Pd] = 3.3, pH 3.8) was recorded. As a result, the shape of the XA spectrum for the Pd-ISA solution ([ISA]/[Pd] = 3.3, pH 3.8) was the same as that for the $[PdCl_4]^{2-}$ solution (as not shown). The formation of the aqueous Pd-ISA complex is thought to involve any hydroxyl group of ISA, but not the carboxyl group.

3.3 FTIR Analysis of ISA in the Presence of Pd

Figure 6 shows the FTIR spectrum of the 0.1 mol·dm^{-3} ISA stock solution (pH 10.0) and Pd-ISA solution at pH ranging from 8.5 to 12.5. As no precipitation was visually observed in the solution before measurement, Pd is expected to be present in the solution forming Pd-ISA complexes. The spectrum of the ISA stock solution has many characteristic peaks; however, we focused on the peaks at 1583, 1413, and 1000–1150 cm^{-1}, corresponding to the asymmetric stretching vibration of the carboxylate group (ν_{as} (COO^-)), symmetric stretching vibration of the carboxylate group (ν_s (COO^-)), and binding vibration of C-OH (alcohol) (ν(C-OH)), respectively [15].

Consequently, a decrease in the absorption of ν_{as} (COO^-) and ν_s (COO^-) was observed in the comparison of the ISA solution spectrum with that of Pd, which suggested that the carboxyl group in the ISA structure contributed to the formation of the Pd-ISA complex. Because the spectrum of the Pd-ISA solution at pH 8.5 is similar to that at pH 10.0, the Pd-ISA complex appears to be present in both solutions in the same chemical form. Conversely, the peak shift of ν_s (COO^-) to a low wave number was observed at pH 12.5, which is attributed to the complexation with Pd. ISA contains two hydroxyl groups in its

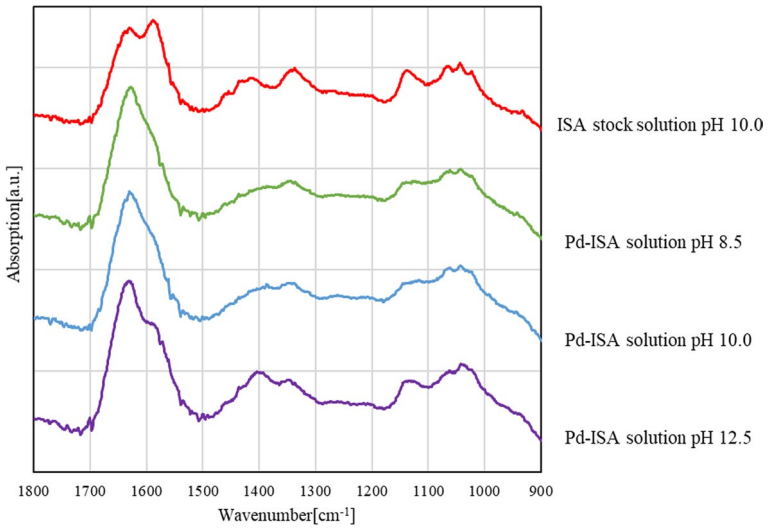

Fig. 6 ATR–FTIR spectra of ISA stock solution and Pd-ISA solutions at different pH values (Pd: 0.006 mol·dm^{-3}; ISA: 0.006 mol·dm^{-3})

molecular structure, which are thought to dissociate at high pH. Therefore, the coordination state between the carboxyl group and Pd possibly changed at pH 12.5. In addition, hydroxide Pd could have been involved in the Pd-ISA complex under such high pH conditions. In contrast, XAFS measurements showed that the coordination structure of Pd did not change at pH 8.5–12.5; however, focusing on the chemical structure of functional groups of ISA, it is predicted that Pd-ISA complexes have a similar coordination state at pH 8.5–10, whereas the contribution of OH^- appears at pH 12.5.

3.4 Thermodynamic Interpretation of Pd(II) Solubility in the Presence of ISA

The comparison of XAFS analysis in this work confirmed that Pd tends to form complexes with ISA in the pH range of 8.5–12.5. Moreover, it was suggested that not only the carboxyl groups but also the hydroxyl groups in the ISA structure contribute to the formation of a complex with Pd(II). Similarly, it was suggested that the chemical form of the Pd-ISA complex depends on the solution pH; specifically, the number of involved OH^- ions should be changed by solubility experiments and FTIR analysis. Based on these results, the equilibrium reaction Eq. 1, the hydrolysis reaction Eq. 2, and the complexation reaction Eqs. 3–5 are proposed to control the solubility of Pd(II) in the presence of ISA. The solubility constants of Eqs. 1–5 are described by Eqs. 6–10, where the subscript of constants is indicating the number of Pd(II), OH^-, and ISA^-, respectively.

$$\mathrm{Pd(OH)_2}(am) \iff \mathrm{Pd(OH)_2}(aq) \tag{1}$$

$$\mathrm{Pd^{2+}} + 3\mathrm{H_2O} \iff \mathrm{Pd(OH)_3^-} + 3\mathrm{H^+} \tag{2}$$

$$\mathrm{Pd(OH)_2}(am) + \mathrm{ISA^-} + \mathrm{H^+} \iff \mathrm{PdOHISA}(aq) + \mathrm{H_2O}(l) \tag{3}$$

$$\mathrm{Pd(OH)_2}(am) + \mathrm{ISA^-} \iff \mathrm{Pd(OH)_2ISA^-} \tag{4}$$

$$\mathrm{Pd(OH)_2}(am) + \mathrm{ISA^-} + \mathrm{H_2O}\ (l) \iff \mathrm{Pd(OH)_3ISA^{2-}} + \mathrm{H^+} \tag{5}$$

with

$$\log_{10}K'_{s,(1,2,0)} = \log_{10}\left[\mathrm{Pd(OH)_2}(aq)\right] \tag{6}$$

$$\log_{10}K'_{s,(1,3,0)} = -(15.48 \pm 0.35)[3], \tag{7}$$

$$\log_{10}K'_{s,(1,1,1)} = \log_{10}\left[\mathrm{PdOHISA}(aq)\right] - \log_{10}[\mathrm{ISA^-}] - \log_{10}\left[\mathrm{H^+}\right], \tag{8}$$

$$\log_{10}K'_{s,(1,2,1)} = \log_{10}\left[\mathrm{Pd(OH)_2ISA^-}\right] - \log_{10}[\mathrm{ISA^-}], \tag{9}$$

$$\log_{10}K'_{s,(1,3,1)} = \log_{10}\left[\mathrm{Pd(OH)_3ISA^{2-}}\right] + \log_{10}\left[\mathrm{H^+}\right] - \log_{10}[\mathrm{ISA^-}]. \tag{10}$$

For the determination of conditional equilibrium constants, slope analysis of solubility curves ($\log_{10}$[Pd] vs. $\log_{10}$[ISA] of different pH and ionic strength), obtained by the solubility experiment, was performed. In this study, the SIT was adopted to account for ion

interaction processes and ionic strength effects [16]. Within the SIT formalism, activity coefficients γ_j are calculated accordingly:

$$\log_{10}\gamma_j = -z_j{}^2 D + \sum_k \epsilon\left(j,k,I_m\right)m_{k,} \tag{11}$$

where D represents the Debye–Hückel term, z_j the charge of anion j, I_m the molal ionic strength, m_k the molality of all ions k present in the solution, and (j, k, I_m) the specific ion interaction parameter. Solubility experiments were conducted using 0.1 and 0.6 mol·dm^{-3} NaCl–NaOH with NaISA; therefore, the extrapolation to $I=0$ mol·dm^{-3} was performed using the following SIT coefficients:

$\varepsilon(H^+, Cl^-) = 0.12 \pm 0.01$ kg mol^{-1} (adopted from Rand et al. [17])
$\varepsilon(Pd(OH)_3{}^-, Na^+) = 0.11$ kg mol^{-1} (estimated by Rai et al. [12])
$\varepsilon(ISA^-, Na^+) = -(0.07 \pm 0.01)$ kg mol^{-1} (in analogy to Hox-, as proposed by Hummel et al. [8])
$\varepsilon(PdOHISA(aq), Na^+/Cl^-) = 0$ (by the definition in SIT).
$\varepsilon(Pd(OH)_2ISA^-, Na^+) = -(0.05 \pm 0.10)$ kg mol^{-1} (estimated from charge analogy [18])
$\varepsilon(Pd(OH)_3ISA^{2-}, Na^+) = -(0.10 \pm 0.10)$ kg mol^{-1} (estimated from charge analogy [18])

Consequently, the stability constants of each Pd-ISA complex at $I=0$ mol dm^{-3} were calculated using Eqs. (6)–(8) and the following parameters:

$$\log_{10}K^{\circ}{}_{s,(1,1,1)} = \log_{10}K'{}_{s,(1,1,1)} + \log_{10}\gamma_{PdOHISA(aq)} + \log_{10}a_w - \log_{10}\gamma_{ISA^-} - \log_{10}\gamma_{H^+} \tag{12}$$

$$\log_{10}K^{\circ}{}_{s,(1,2,1)} = \log_{10}K'{}_{s,(1,2,1)} + \log_{10}\gamma_{Pd(OH)_2ISA^-} - \log_{10}\gamma_{ISA^-} \tag{13}$$

$$\log_{10}K^{\circ}{}_{s,(1,3,1)} = \log_{10}K'{}_{s,(1,3,1)} + \log_{10}\gamma_{Pd(OH)_3ISA^{2-}} + \log_{10}\gamma_{H^+} - \log_{10}\gamma_{ISA^-} - \log_{10}a_w \tag{14}$$

Rai et al. reviewed the reports of Middlesworth et al. [10] and Oda et al. [11] and then recommended the solubility constants of $Pd(OH)_2$ (am) as $\log_{10}K^{\circ}_{s,0} = -3.58$ and the equilibrium constant for the formation of $Pd(OH)_2$(aq) as $\log_{10}K^{\circ}_{(1,2,0)} < -3.49$ [12], which is defined by following Eqs. (15), (16):

$$Pd(OH)_2(am) + 2H^+ \iff Pd^{2+} + 2H_2O, \tag{15}$$

$$Pd^{2+} + 2H_2O \iff Pd(OH)_2(aq) + 2H^+. \tag{16}$$

The logarithm of equilibrium aqueous concentration of $Pd(OH)_2$(aq) (the value of Eq. (6)), which is calculated by the addition of $\log_{10}K^{\circ}_{s,0}$ and $\log_{10}K^{\circ}_{(1,2,0)}$, should be -7.07. However, some plots of soluble Pd concentration in the solubility experiment were smaller than 10^{-7} mol·dm^{-3} even in the presence of ISA mentioned above. For a better interpretation of experimental results, we used the value of $\log_{10}K^{\circ}_{(1,2,0)} < -5.42$, which is based on the reported value by Oda et al. [11]. Then, the value of Eq. (6) is considered to be 9.00 and used in the fitting in this study.

The fit of solubility data in the presence of ISA at $I=0.1$ and 0.6 mol·dm^{-3}, along with the chemical model proposed above, could reproduce all experimental data collected in this study well. The fitting results (a) $\log_{10}$[Pd] vs. $\log_{10}$[ISA] at $I=0.1$ mol·dm^{-3}, (b) $\log_{10}$[Pd] vs. $\log_{10}$[ISA] at $I=0.6$ mol·dm^{-3}, and (c) $\log_{10}$[Pd] vs. pH values at $I=0.6$ mol·dm^{-3} are

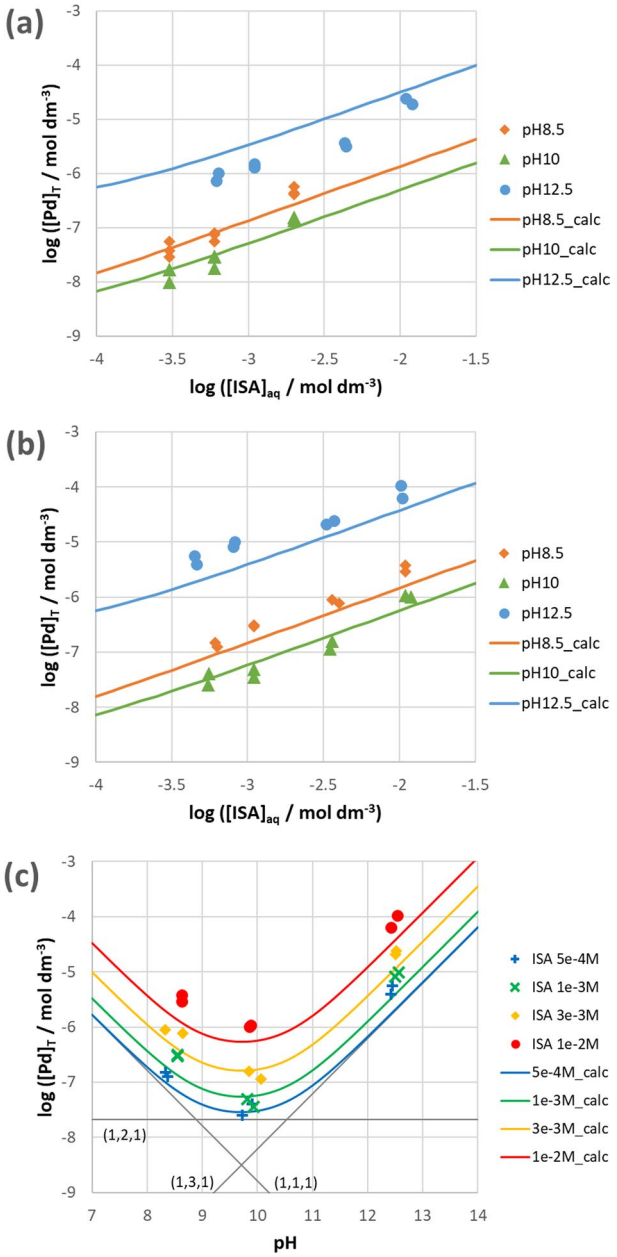

Fig. 7 Experimental Pd(II) solubility data for **a** $\log_{10}$[Pd] vs. $\log_{10}$[ISA] at $I = 0.1$ mol·dm^{-3}, **b** $\log_{10}$[Pd] vs. $\log_{10}$[ISA] at $I = 0.6$ mol·dm^{-3}, and **c** $\log_{10}$[Pd] vs. pH at $I = 0.6$ mol·dm^{-3}. The thick lines correspond to the calculated results with the thermodynamic model derived in this work ($R^2 = 0.934$). The thin lines indicate aqueous speciation(at [ISA] $= 5 \times 10^{-4}$ mol·dm^{-3})

depicted in Fig. 7. In this fitting, all experimental data were fitted using the nonlinear least squares method, where $\log_{10} K^{o}_{s,(1,n,1)}$was used fitting parameters. These results indicate that complexation with ISA can increase the solubility of $Pd(OH)_2$ (am) by approximately two orders of magnitude compared with the reported conditional value of the solubility of Pd in the ISA-free system.

The estimated values and standard deviations are as follows:

Table 2 Stability constants for the solubility of Pd(II) and the formation of ISA complexes as derived in the present work (p.w.) or reported by Rai et al. [12]

		Reference
Solubility	$\log_{10}K^{o}_{s,0}$	
$Pd(OH)_2(am) + 2H^+ \iff Pd^{2+} + 2H_2O$	$-(3.58 \pm 0.36)$	Rai et al. [12]
ISA complexes	$\log_{10}K^{o}_{(1,n,1)}$	
$Pd^{2+} + H_2O(l) + ISA^- \iff PdOHISA(aq) + H^+$	8.1 ± 0.4	(p. w.)
$Pd^{2+} + 2H_2O(l) + ISA^- \iff Pd(OH)_2ISA^- + 2H^+$	$-(0.8 \pm 0.4)$	(p. w.)
$Pd^{2+} + 3H_2O(l) + ISA^- \iff Pd(OH)_3ISA^{2-} + 3H^+$	$-(11.4 \pm 0.4)$	(p. w.)

$$\log_{10}K^{o}{}_{s,(1,1,1)} = (4.5 \pm 0.1)$$

$$\log_{10}K^{o}{}_{s,(1,2,1)} = -(4.4 \pm 0.1)$$

$$\log_{10}K^{o}{}_{s,(1,3,1)} = -(15.0 \pm 0.1)$$

.

González-siso et al. conducted a solubility experiment of Ni(II) in the absence and presence of ISA and determined the conditional equilibrium constants of NiOHISA(aq), $Ni(OH)_2ISA^-$, and $Ni(OH)_3ISA^{2-}$ as 5.6 ± 0.3, $-(5.5 \pm 0.5)$, and $-(18.9 \pm 0.7)$, respectively [19]. This result indicates the similarity between Pd and Ni as d^8 transition metal ions, which tend to form planar structures even in complexation with ISA. These elements have low solubility because of the strong affinity of hydrolysis in neutral to alkaline pH; therefore, the impact of complexation with ISA in the safety assessment of the disposal of radioactive wastes should be remarkable in the presence of millimole order of ISA.

The combination of $\log_{10}K^{o}_{s,(1,n,1)}$ (n = 1–3) in this study and $\log_{10}K^{o}_{s,0}$, estimated by Rai et al., enables the calculation of the equilibrium constants for the formation of the complexes PdOHISA(aq), $Pd(OH)_2ISA^-$, and $Pd(OH)_3ISA^{2-}$ ($\log_{10}K^{o}_{(1,n,1)}$), as summarized in Table 2. Hence, the thermodynamic models and conditional parameters for the thermodynamic calculation of Pd(II) solubility in waste disposal were derived in this study.

4 Conclusions

The solubility of Pd(II) under neutral to alkaline pH conditions was increased by approximately two orders of magnitude in the presence of ISA compared with the reported conditional value of Pd solubility in an ISA-free system. Aqueous Pd and ISA were investigated by XA spectroscopy and FTIR, respectively. As a result, it was suggested that Pd tends to form a complex with ISA under neutral to alkaline pH conditions and that the chemical form of the Pd-ISA complex depends on pH. Specifically, the contribution of hydroxyl ions was observed at pH 12.5. Accordingly, the thermodynamic models and the conditional complexation constants of Pd with ISA were estimated by the slope analyses of the solubility experiment results. The similarity between the thermodynamic models and equilibrium constants of Pd(II) and Ni(II) with ISA was revealed. Hence, the impact of complexation

with ISA on Pd(II) solubility under disposal conditions could be calculated using the proposed chemical and thermodynamic models.

Supplementary Information The online version contains supplementary material available at https://doi.org/10.1007/s10953-023-01352-6.

Acknowledgements This study was conducted as a part of R&D supporting program titled "Advanced technology development for geological disposal of TRU waste (2022 FY)" under the contract with Ministry of Economy, Trade and Industry (METI) (Grant Number: JPJ007597).

Author Contributions SK contributed toward conceptualization, methodology, writing—original draft, and writing—review and editing. YT contributed toward writing—original draft. HI contributed toward conceptualization, methodology, and writing—review and editing. TI contributed toward conceptualization and writing—review and editing. AK contributed toward conceptualization, methodology, and writing—review and editing. YT contributed toward supervision and writing—review and editing. TT contributed toward methodology, investigation (sample preparation, solubility experiments, and FT-IR), and writing—review and editing. KH contributed toward methodology, and investigation (sample preparation, solubility experiments, and FT-IR). MH contributed toward methodology, and investigation (XA spectroscopy). SM contributed toward conceptualization, and methodology. DK contributed toward methodology, investigation (XA spectroscopy), writing—original draft, and writing—review and editing.

Declarations

Competing interests The authors declare no competing interests.

References

1. The Nuclear Waste Management Organization of Japan (NUMO): : The NUMO Pre-siting SDM-based Safety Case., NUMO-TR21-01, (2021). https://www.numo.or.jp/technology/technical_report/pdf/NUMO-TR21-01_rev220222.pdf Accessed 8 June 2023
2. Glaus, M.A., Van Loon, L.R.: Degradation of cellulose under alkaline conditions: New insights from a 12 years degradation study. J. Environ. Polym. Degrad. **42**, 2906–2911 (2008)
3. Glaus, M.A., Van Loon, L.R., Schwyn, B., Vines, S., Williams, S.J., Larsson, P., Puigdomenech, I.: Long-term prediction of the concentration of a-isosaccharinic acid in cement pore water. Mater. Res. Soc. Symp. Proc. **1107**, 605–612 (2008)
4. Greenfield, B.F., Holtom, G.J., Hurdus, M.H., et al.: The identification and degradation of isosaccharinic acid, a cellulose degradation product. Mater. Res. Soc. Symp. Proc. **353**, 1151–1158 (1995)
5. Tits, J., Wieland, E., Bradbury, M.H.: The effect of isosaccharinic acid and gluconic acid on the retention of Eu(III), am(III), and th(IV) by calcite. Appl. Geochem. **20**, 2082–2096 (2005)
6. Moreton, A.D., Pilkington, N.J., Tweed, C.J.: Thermodynamic modeling of the effect of hydroxycarboxylic acid on the solubility of plutonium at high pH. UK NIREX Report NSS/R399, UK (2000)
7. Kobayashi, T., Sasaki, T., Kitamura, A.: Thermodynamic interpretation of uranium (IV/VI) solubility in the presence of a-isosaccharinic acid. J. Chem. Thermodynamics. **138**, 151–158 (2019)
8. Hummel, W., Anderegg, G., Puigdomenech, I., Rao, L., Tochiyama, O.: Chemical thermodynamics of compounds and complexes of U, Np, Pu, Am, Tc, Se, Ni and Zr with selected organic ligands. Chemical Thermodynamics Series Vol. 11, Nuclear Energy Agency in Organization for Economic Co-operation and Development (OECD/NEA), (2005)

9. Baes, C.F., Mesmer, R.E.: The Hydrolysis of Cations. Krieger, Florida (1986)
10. Middlesworth, J.M., Wood, S.A.: The stability of palladium(II) hydroxide and hydroxy-chloride complexes: An experimental solubility study at 25–85℃ and 1 bar. Geochim. Cosmochim. Acta. **63**(11/12), 1751–1765 (1999)
11. Oda, C., Yoshikawa, H., Yui, M.: Effects of aging on the solubility of palladium. Mat. Res. Soc. Symp. Proc. **412**, 881–887 (1996)
12. Rai, D., Yui, M., Kitamura, A.: Thermodynamic model for amorphous $pd(OH)_2$ solubility in the aqueous Na^+-K^+-H^+-OH^--Cl^--ClO_4^--H_2O system at 25℃: A critical review. J. Solution Chem. **41**, 1965–1986 (2012)
13. Rai, D., Kitamura, A.: Thermodynamic equilibrium constants for important isosaccharinate reactions: A review. J. Chem. Thermodynamics. **114**, 135–143 (2017)
14. Ravela, B., Newville, M.: ATHENA, ARTEMIS, HEPHAESTUS: Data analysis for X-ray absorption spectroscopy using IFEFFIT. J. Synchrotron Rad. **12**, 537–541 (2005)
15. Brinkmann, H., Patzschke, M., Kaden, P., Raiwa, M., Rossberg, A., Kloditz, R., Heim, K., Moll, H., Stumpf, T.: Complex formation between UO_2^{2+} and a-isosaccharinic acid: Insights on a molecular level. Dalton Trans. **48**, 13440–13457 (2019)
16. Ciavatta, L.: The specific interaction theory in evaluating ionic equilibria. Ann. Chim. **70**, 551–567 (1980)
17. Rand, H.M., Fuger, J., Grenthe, I., Neck, V., Rai, D.: Chemical Thermodynamics of Thorium. Nuclear Energy Agency in Organization for Economic Co-operation and Development. OECD/NEA), Paris (2008)
18. Hummel, W.: Ionic strength corrections and estimation of SIT ion interaction coefficients, Paul Scherrer Institute, PSI report TM-44-09-01 (2009)
19. González-Siso, M.R., Gaona, X., Duro, L., Altmaier, M., Bruno, J.: Thermodynamic model of Ni(II) solubility, hydrolysis and complex formation with ISA. Radiochim. Acta. **106–1**, 31–45 (2017)